Invited Review:
Emission Lines and the High Energy Continuum

To appear in Quasars as Standard Candles for Cosmology*, eds. J. Baldwin & G. Ferland (San Francisco: Astronomical Society of the Pacific), in press*

Paul J. Green

Harvard-Smithsonian Center for Astrophysics, 60 Garden St., Cambridge, MA 02138

Abstract. Quasars show many striking relationships between emission line and continuum radiation. The physical origin of these diverse and interrelated correlations has yet to be determined. We take as an example the observed anticorrelation between emission line equivalent width and underlying continuum luminosity (the Baldwin Effect). We examine mechanisms that might account for 4 particularly intriguing characteristics of the Baldwin Effect. In nearly every case, more than one such mechanism must be invoked. We argue that the most promising mechanism is that the spectral energy distribution (SED) of the overall quasar continuum changes with luminosity, driving emission lines differently depending on their effective ionization energies. Several lines of evidence point to the sobering fact that the SEDs we observe are not those impinging on the emission line clouds, but instead may be strongly affected by (both neutral and ionized) absorption and by scattering. Interpretation of the data is complicated because, even in assumed flattened geometries, the standard accretion disk, broad emission line region, molecular torus, and narrow emission line region are not necessarily aligned. A multiwavelength approach with particular attention to the interplay of absorption and emission shows promise for significant advances in our understanding.

1. Introduction

Quasars, the most distant, most luminous objects in the Universe, are proving more useful than ever imagined for reaching toward the edge of cosmic time, for illuminating the intervening matter, and for probing extremes of physics. Though most of the nearly 10,000 QSOs now known were *discovered* by their unique spectral energy distributions (SEDs) and emission lines, these fundamental questions demand to be addressed:

1) What is the true shape of the SEDs ?
2) What effect does the continuum have on emission lines?
3) How are both of these affected by intrinsic absorption and orientation?

1.1. The Ionizing Continuum

The spectral energy distributions (SEDs) of quasars are roughly homogeneous, extending from the infra-red to the hard X-rays. The simplest model that explains the overall continuum production is energy release from an accretion disk around a massive blackhole. The optical/UV "big blue bump" (BBB), commonly observed in quasar spectral energy distributions (SEDs; e.g., Elvis et al. 1994) as an upturn in emission toward shorter wavelengths, is attributed to the thermal accretion disk (see Figure 1). The X-ray 'soft excess' (soft X-ray emission that exceeds the extrapolation from the observed hard X-ray power-law continuum; Masnou et al. 1992) has often been interpreted as the high energy continuation of the BBB, possibly thermal emission from the inner accretion disk (although see Barvainis 1993). Somewhere in the extreme ultraviolet (EUV) band, the SEDs peaks and turn down again to meet the observed X-ray emission.

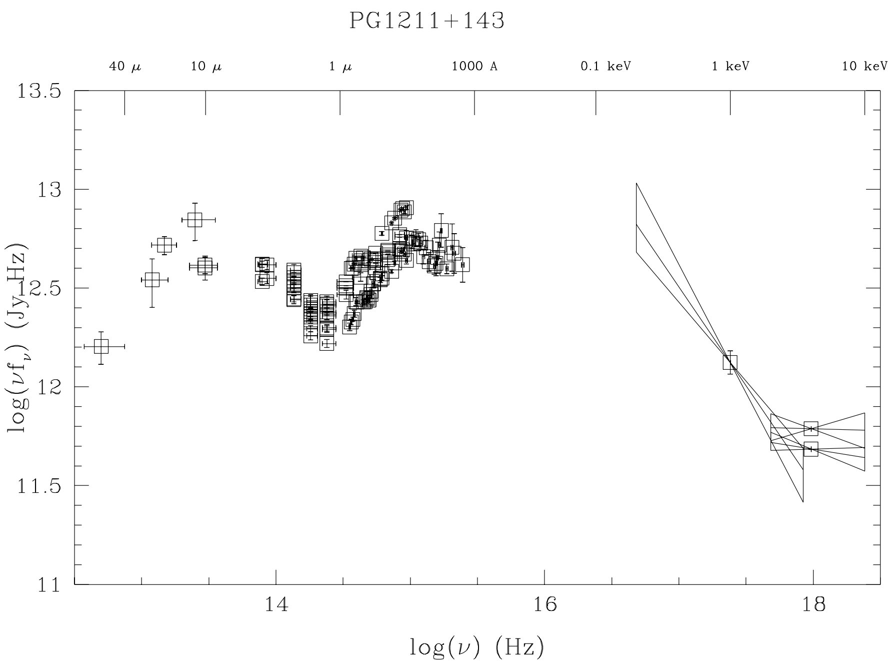

Figure 1. The spectral energy distribution (SED) for a representative QSO, PG1211+143 (Elvis et al. 1994). The OUV and X-ray regions that contribute to the BBB are marked in the figure. Perhaps the most obvious feature in this typical SED is the gap in coverage in the EUV, due to obscuration. Continuum slopes can now be reliably measured in the UV/soft X-ray bands for large numbers of QSOs with HST, and ROSAT, making estimates of EUV strength feasible. Such measurements are critical since the EUV contains a large fraction of the total bolometric luminosity of QSOs, and dominates UV emission line production.

The production of emission lines in QSO spectra is widely attributed to photoionization and heating of the emitting gas by the UV to X-ray continuum (e.g., Ferland & Shields 1985; Krolik & Kallman 1988 - KK88). Emission lines from a given ion are particularly sensitive to photons of energy above the corresponding ionization threshold. As an example, the continuum flux relevant to the production of Lyα emission is above 13.6eV, while He IIλ1640 is produced by photons above the 54eV ionization edge of He$^+$, which at 228Å is in the EUV. Note however that the production of many emission lines may be sensitive to continuum energy ranges both softer and harder than the ionization potential of the species in question, because such photons may ionize from excited states and also heat the gas via free-free and H$^-$ absorption. Many important lines are driven by the extreme ultraviolet (EUV) or soft X-ray continuum. Unfortunately, the EUV band is severely obscured by Galactic absorption. However, some constraints on the EUV ionizing continuum are available through analysis of the adjacent UV and soft X-ray windows.

The overall similarity of QSO emission line spectra had been taken as evidence of fairly uniform, robust physical conditions in the broad emission line region (BELR). At first, this encouraged the assumption that clouds in the BELR inhabit a narrow swath of parameter space (in density, size, and ionization). Photoionization pioneers such as Mushotsky & Ferland (1984) ran models on a single cloud. Refinements using cloud ensembles yield more robust and realistic predictions for line emission (Binette et al. 1989, Baldwin et al. 1995). However, many observed correlations of emission line properties with SEDs remain mysterious, and present a challenge to geometric and photoionization models that needs to be answered.

2. The Dependence of Emission Line Strength on Luminosity

During the exuberant early years since the discovery of AGN, many published studies touted as remarkable that QSO luminosities measured in different bandpasses were well correlated over a large range of luminosity. This was cited as evidence for physically linked intrinsic emission mechanisms from radio through X-ray wavelengths. One of the first pillars of evidence for photoionization as the main excitation mechanism of emission lines in active galaxies was the strong correlation of emission line luminosity with continuum luminosity. However, the strong influence of distance-scaling on luminosities nearly guarantees such results in the typically flux-limited surveys used (Kennicut 1990), particularly since non-detections are often neglected.

Because the simplest photoionization models predict a linear proportionality between line and continuum strength, diagnostics such as line ratios and equivalent widths (the ratio of integrated line flux over local continuum flux density) should be *independent* of continuum luminosity. Baldwin (1977) first noticed that in high redshift quasars, the CIV λ1550Å emission line equivalent width (W_λ hereafter) in quasars *decreases* with increasing UV (1450Å) luminosity. Since flux *ratios* are distance-independent, this discovery brought hope that, regardless of its physical explanation, the Baldwin Effect might enable QSOs to be used as a "standard candle" in measuring cosmological distances.

The very large dispersion in this anticorrelation (e.g., Zamorani et al. 1992) still yields poor distance calibrations relative to other standard candles. Relative luminosity distances accurate to 10% at $z \sim 0.5$ and 20% at $z = 1$ are becoming possible with new Type 1a supernova measurements (e.g. Garnavich et al. 1998; Hamuy et al. 1996; Suntzeff or Tytler, this volume). COBE, Planck, and MAP should tightly constrain cosmological models (Tytler, this volume). Undaunted, we continue to pursue a deeper understanding of the Baldwin Effect for several reasons. First, QSOs represent by the majority of the most distant measurable objects in the Universe, extending to $z = 5$. Second, we expect the Baldwin Effect to harbor some important information on the QSOs themselves. Substantial reduction in the scatter is not critical to use of the Baldwin Effect for cosmology, as long as we can show that the sources of scatter are the same at all redshifts. But if we can understand the origin of the Baldwin Effect and the source(s) of scatter, we will have learned more about the intrinsic QSO physics.

Several relevant characteristics of the Baldwin Effect have been noted that must be accounted for in physical models.

A) The Baldwin effect (BEff, hereafter) is strong not only for CIV, but also for ions such as OVI, NV, He II, CIII], Mg II, and Lyα (e.g., Tytler & Fan 1992, Zamorani et al. 1992). In all cases, I will refer to slopes in the log-log domain of equivalent width W_λ vs. luminosity L. Thus, a slope β_w describes $W_\lambda \propto L^{\beta_w}$. Typical slopes for CIV are $\beta_w \sim -0.2$ (Kinney, Rivolo, & Koratkar 1990). [1] The ensemble BEff has steeper slopes for lines of higher ionization energy (Zheng, Fang, & Binette 1992; Espey, this volume).

B) The ensemble BEff shows steeper slopes for subsamples of smaller luminosity range (Netzer, Laor, & Gondhalekar 1992).

C) The component of emission lines that changes the most with luminosity in samples of QSOs has a narrow FWHM (Osmer, Porter & Green 1993).

D) There is a BEff *intrinsic* to individual objects as they vary such that, when their continuum varies, the attendant line emission varies by a smaller amount. For CIV, this corresponds to $\beta_w \sim -0.7$ (Kinney et al. 1990). The steep slope of the intrinsic BEff itself adds considerable scatter to the shallower ensemble BEff, unless suitably averaged data are used for every object. The intrinsic BEff probably persists even into the hard X-ray regime (for the Fe Kα emission line; Iwasawa & Taniguchi 1993) In the UV, the removal of light-travel time effects in the broad-line region reduces scatter in the intrinsic effect (Pogge & Peterson 1992).

2.1. Prevailing Mysteries in Line/Continuum Correlations

Just as all QSO samples suffer from selection effects and biases, so inevitably will this review. The clues and puzzles in line/continuum correlations that I review in this article include several dear to many in the AGN guild, and are discussed elsewhere in this volume.

- What causes the non-linear relationship between line and continuum luminosity (the Baldwin Effect)?

[1] Some studies characterize the relationships as $W_\lambda \propto M_V^{\beta_m}$ ($\beta_m = -0.4\beta_w$; Zamorani et al. 1992, Zheng, Fang, & Binette 1992), or $L_{line} \propto L^\beta$ (($\beta = 1 + \beta_w$; Pogge & Peterson 1992).

- Why do profound apparent differences in SED sometimes result in at best small differences in emission line properties e.g., broad absorption line (BAL) QSOs?
- Why do some line transitions of a give species appear to correlate with high energy emission, while others anticorrelate (FeII)?
- How do we resolve the "photon deficit"?
- Is there a physical interpretation for the ensemble of correlations (better known as "Eigenvector 1") that account for the bulk of QSO optical spectral diversity?

Rather than answer all these questions, I'm forced to merely sketch their origin, my current state of understanding, and some possible directions toward resolution.

My emphasis, however, is on the high energy continuum, primarily X-rays. Although the field of high energy astronomy is now decades old, the difficulty of space-based X-ray observations - small apertures, low spectral and spatial resolution - have meant that X-ray astronomy's inherent ability to probe high ionization states, high temperatures, and regions nearest the nucleus have remained relatively limited. X-ray satellites to be launched in the next several years will overcome many of those limitations, and rapidly unveil corners of parameter space yet unexplored.

3. Possible Causes of the Baldwin Effect

Several physical mechanisms have been offered to explain the Baldwin Effect: 1) Orientation of a thin accretion disk. 2) Variability effects. 3) Optically thin emitting clouds. 4) Changes in covering fraction with luminosity. 5) Shifts of the SED with luminosity. These may act in some linear combination (depending on the nature of the sample and observations) to produce the BEff itself, and/or to introduce scatter. A speedy review of the first 4 will have to suffice before I detail the evidence for the last.

3.1. Orientation

Optically thick, geometrically thin accretion disk models with no corona (e.g., Netzer et al. 1992 and references therein) have successfully explained several line/continuum correlations. Limb darkening and projected surface area effects call for a UV continuum flux that is strongest face-on, and highly anisotropic compared to the harder (e.g., soft X-ray) ionizing flux. Quasar disks, particularly the area emitting the UV flux, are much smaller than the BELR (assumed to be a spherical shell). Thus a random selection of objects, differing only in disk inclination, results in measurements of constant line luminosities but yields UV continuum luminosities that vary with aspect, thereby producing the observed anticorrelation between W_λ and L_{UV}. If indeed X-ray emission is more isotropic, much weaker correlations would be observed between W_λ and L_X. In addition, disks viewed face-on (smaller W_λ) would also appear to have boosted UV (larger α_{ox}).

All of the predictions of the orientation model appear to hold true for the Lyα line (Netzer et al. 1992, Green 1996). However, the model predicts the same set of correlations with CIV, whereas a corresponding decrease of W_λ(C IV) with α_{ox} is ruled out (Green 1996). The simplest orientation model of the BEff also appears to be contradicted by the finding of a dominant anti-correlation between W_λ(C III]) and X-ray luminosity. Predictions for CIV correlations and W_λ distributions disagree quantitatively with those observed (Francis 1993). Line/continuum correlations examined by Wilkes et al. (1998), however, may favor the model.

Disk inclinations only predict a range in observed L_{UV} of at most a factor 10 at a given isotropic luminosity, and they appear to reproduce the steep slopes of the *intrinsic* BEff. The orientation models of Netzer et al. (1992) quite reasonably invoke a range of isotropic luminosities (corresponding to a range of black holes masses M_{BH} and accretion rates $\dot{M}$), which populates the entire ensemble BEff diagram, yielding both slope and scatter close to that observed, at least for Lyα. Because AGN disks surely do not jiggle on human timescales, disk inclinations alone clearly can *not* account for the *intrinsic* BEff, without invoking at least one of the other mechanisms. Given the simplicity of the models used[2] the lesson that orientation effects may well add scatter to the ensemble BEff is well-taken.

3.2. Variability

Strong continuum variability, with smaller line variability can reproduce the intrinsic BEff. The finite light-crossing time of the BELR might partly induce the intrinsic BEff by smoothing the line response to continuum variability (e.g., Edelson, Pike & Krolik 1990). However, removal of medium-term (4-20d) lags by comparing line emission to lag-corrected continuum reduces scatter, but does not change the slope of the intrinsic BEff in Seyferts (Pogge & Peterson 1992). Over the small range in L covered by intrinsic variability, a steep slope β_w is expected.

Continuum variations intrinsic to individual quasars have the attraction of involving fewer parameters, since disk inclination, M_{BH} and covering fraction are effectively constant. The intrinsic BEff, at least, must be explainable without invoking these, leaving virtually only $\dot{M}$, concomitant SED changes, and cloud properties with which to fiddle.

Variability probably anticorrelates with luminosity in AGN, so that the phenomenon is unlikely to persist in high L QSOs. In any case, the ensemble BEff over a larger range in L (particularly when using averaged multi-epoch spectra) would not be reproduced by variability, without invoking at least one of the other mechanisms.

3.3. Optically thin clouds

At least in Seyferts, broad line emission has been observed to saturate when the continuum is in a high phase (e.g., Wamsteker & Colina 1986 for the case of

[2] No changes in covering fraction, multiple cloud zones, or changes in ionization parameter U as a function of inclination were considered.

Fairall 9; Ferland, Korista & Peterson 1990 for Mrk 590). A flat or even *negative* correlation between continuum flux and line emission for a given species can result for fully ionized clouds, as the dominant ionization state of the element changes.

The so-called "warm absorbers" illustrate this phenomenon. Soft X-ray absorption in AGN shows apparent (cold) column densities that *decrease* with increasing continuum luminosity in individual, variable AGN (Halpern 1984, Otani et al. 1996). The predominant absorbing species (highly ionized oxygen, OVII and OVIII in soft X-rays) are "ionized away" by an increasing ionization parameter.[3]

In MCG-6-30-15, although the OVIII absorption varies strongly the depth of the OVII edge shows no response to the continuum flux, indicating that it originates in gas at larger radii (Otani et al. 1996). The X-ray results suggest that the warm absorbers span regions near or within the BELR, while the less ionized absorbers are further out, perhaps associated with the outer molecular torus, scattering medium, or NELR.

Optically thin absorbing clouds, when not along the line-of-sight to the continuum source, will also give rise to emission lines. Optical/UV low-ionization lines (LILs) originate at characteristically larger distances from the central source than high ionization lines (HILs), and may indeed be associated with the warm absorbers.

As proposed by Shields, Ferland & Peterson (1995), optically thin clouds can thus account at least qualitatively for some of the phenomena related to the intrinsic BEff cited above (see also Shields, this volume). One would expect the optically thin clouds to dominate closer in to the nucleus, and therefore be associated with the broad line component. This may contradict observations showing that the ensemble BEff is dominated by narrow components (Osmer et al. 1993). To account for the ensemble BEff's steeper slopes for subsamples of smaller luminosity range, however, requires invoking at least one of the other mechanisms.

3.4. Change in Covering Fraction with Luminosity

If higher luminosity AGN have a lower covering fraction (i.e., a smaller fraction of the sky as seen from the nucleus is covered with emitting clouds), then they will also have weaker line emission, causing a BEff. At higher luminosities, the radius at which clouds of constant density n become optimally-emitting (the radius at which ionizing flux U maximizes line flux) for a given species increases (as $L^{1/2}$). This would *increase* the total emission measure of a spherical BLR, and so not cause a BEff. However, a BEff might be expected to result from a *flattened* cloud distribution, since then the angle subtended at the nucleus by emitting clouds at the larger radii would be smaller.

3.5. The SED Model

Traditionally, the BEff is seen when comparing UV emission line to its underlying (UV) continuum luminosity. For some cases we are able to compare line emission

[3]Ionization parameter U is the local ratio of the densities of ionizing photons to nucleons.

more directly to a portion of its ionizing/heating ("driving") continuum using extant soft X-ray observations. For Lyα and CIV, comparisons to L_x show an insignificant BEff (Green 1996). This would suggest that the BEff weakens substantially when the continuum luminosity used for comparison to W_λ is *close* to the driving continuum of the line. For HeII and CIII] lines, the entire driving continuum is *softer* than the soft X-ray bandpass, and a significant BEff persists relative to soft X-ray luminosities. It may be that changes in the normalization of the 'underlying' continuum relative to the driving continuum enhance the traditional BEff.

Observed Shifts of the SED with Luminosity The shape of the continuum (i.e., the SED) of quasars does appear to correlate with luminosity. In the X-ray bandpass, the largest, most uniform study to date – ROSAT All-Sky Survey observations of the Large Bright Quasar Survey (LBQS/RASS hereafter; Green et al. 1995) – confirmed earlier reports (e.g., Wilkes et al. 1994, Tananbaum et al. 1986) that α_{ox} [4] increases significantly with luminosity [5] (Figure 2a). There are also hints (e.g., Schartel et al. 1996) that the soft X-ray photon index Γ of QSOs may decrease with redshift (Figure 2b). [6]

Theoretically, SEDs that soften with increasing luminosity have been predicted in a number of scenarios (Sun & Malkan 1989; Haardt & Maraschi 1993). Several workers (beginning with Malkan & Sargent 1982) have proposed as an explanation of the Baldwin Effect that as QSO luminosity increases, the BBB shifts toward lower energies at higher (OUV) luminosities. As QSOs become more luminous in the optical/UV band, they thereby undergo a weaker increase in log L_x, causing the observed increase in α_{ox}. A shift of the BBB to lower energies at higher luminosity also implies that the associated soft X-ray excess should decrease. The apparent hardening of the soft X-ray powerlaw photon spectral index seen in composite ROSAT spectra of LBQS QSOs toward higher redshifts (Figure 2b; Schartel et al. 1996) gibes with this picture. [7]

SED Model Predictions for Line Emission In the SED model, the response of line flux and W_λ depends in a fairly complicated manner on the peak energy of the BBB, on the BBB normalization relative to the powerlaw continuum, and on the driving continuum of the line species in question. The increase in luminosity may primarily be due to an increase in UV/EUV/soft X-ray emission (the BBB) over the underlying power-law continuum. A shift of the BBB toward lower

---

[4]The slope of a hypothetical power law connecting 2500 Å and 2 keV, defined as $\alpha_{ox} = 0.384 \log(\frac{L_{opt}}{L_X})$.

[5]Redshift and luminosity dependence can be hard to disentangle in magnitude-limited surveys, but several recent results, e.g., Wilkes et al. 1994, confirm the primacy of OUV luminosity in the correlation with α_{ox}.

[6]Γ parameterizes the number of X-ray photons as $N(E) = e^{-N_H \sigma_E} N_o E^{-\Gamma}$, where σ_E is the absorption cross-section per H atom for neutral gas. We note that in one common notation (e.g. Wilkes et al. 1994), the X-ray spectral energy index α is defined by $f_\nu \propto \nu^{-\alpha}$ (so that $\alpha = \Gamma - 1$).

[7]However, higher rest-frame energy X-ray emission is observed in most high luminosity objects, so that soft excess may simply shift out of the observed bandpass.

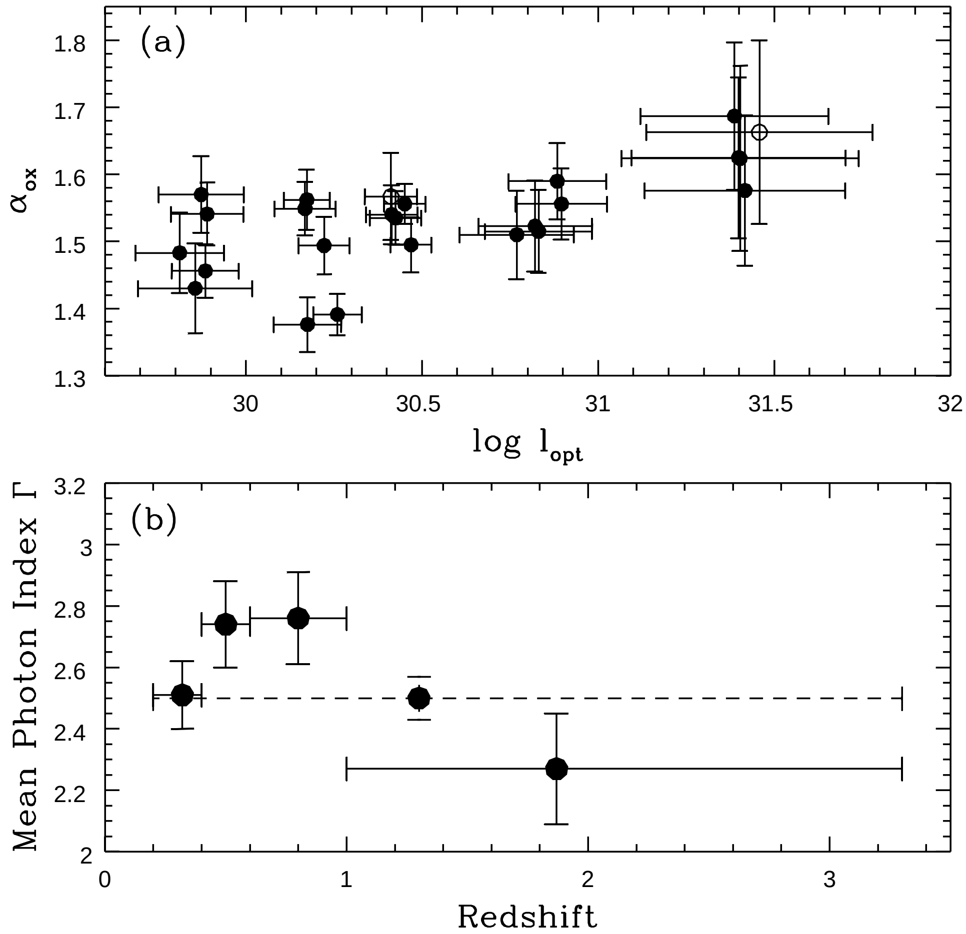

Figure 2. Continuum trends with luminosity and redshift in the LBQS/RASS sample (Green et al. 1995).

energies at higher (OUV) luminosities would entail (1) a strong increase in L_{uv}; (2) a weaker increase in L_x; and (3) an increase in α_{ox}. In the UV regime, Zheng & Malkan (1993) found that the UV continuum increases in strength relative to the optical toward higher luminosities. These trends of continuum shape could strongly influence the efficiency of the driving continuum, and thereby affect observed emission line strengths and ratios. Indeed, Zheng & Malkan found that the strength of the BEff may decrease once the effect of the increasing UV (BBB) continuum is removed.

In the SED picture, a steeper BEff is naturally expected for species of higher ionization energy, since shifts in the relative normalization of their driving and underlying (UV) continuum are then more effective. In fact, it is expected that the correlation between BEff slope and energy should be tightest not with ionization energy *per se*, but rather with the effective energy of the driving continuum. This is borne out in the plots of Espey (this volume).

The intrinsic BEff is compatible with the SED model, since variability of accretion rates in individual AGN would vary the luminosity and SED as well. For the ensemble BEff, if $M_{BH} \propto L$, and the emitting clouds on average have Keplerian velocities, the characteristic velocity of the BELR (corresponding to the emission line FWHM) is $v_{BELR} = (\frac{GM}{R_{BELR}})^{1/2}$. At higher luminosities, the radius at which clouds become optimally-emitting increases $R_{BELR} \propto L^{1/2}$, as appears to be borne out by time-delay sizes inferred from Balmer line lags (Kaspi et al. 1996). Combining these simple expressions leads to a weak *increase* in FWHM with luminosity such that $v \propto L^{1/4}$ (Wandel 1997), whose sense is consistent with the observed trends of linewidth and luminosity (Osmer et al. 1993, Green 1998).

The difference in slope between the intrinsic and ensemble BEff does not arise self-evidently from the SED model. However, the intrinsic effect is most likely due to changes in $\dot{M}$, while the ensemble BEff would be due primarily to differences in M_{BH}. Modelling of the differing resulting SEDs would test whether their expected effects match the observed slope differences. If so, all characteristics are then accounted for, including the steeper BEff for smaller L range.

The shift of SED with luminosity shows promise for accounting for the 4 observed characteristics (A-D) of the BEff discussed here. But is there direct empirical evidence that differences in SED produce changes in emission line properties?

4. Difference Between Optical/UV Spectra of X-ray Bright and X-ray Faint QSOs

Green (1998) contrasted composite optical and UV spectra constructed from samples of QSOs defined by their relative soft X-ray brightness (as determined by α_{ox}). Restframe co-addition (averaging) of spectra with similar continuum properties affords an increase in S/N, and also reduces the effects of variability. To isolate the effects of the SEDs, the samples were chosen to be matched in luminosity and redshift. X-ray bright (XB) composites show stronger emission lines in general, but particularly from the narrow line region. The difference in the [OIII]/Hβ ratio is particularly striking (Figure 3), and even more so when blended FeII emission is properly subtracted. The correlation of this ratio with X-ray brightness were principal components of QSO spectral diversity found by Boroson & Green (1992). Other, much weaker narrow optical forbidden lines (e.g., [OII] and NeV) are enhanced by factors of 2 to 3 in optical XB composites, with narrow line components strongly enhanced in resonance lines of the UV XB composite (Figure 4). Broad permitted line fluxes are slightly larger for all XB spectra, but the narrow/broad line ratio stays similar or increases strongly with X-ray brightness for all strong permitted lines except Hβ. FeII presents an unusual case - the XB composite has stronger UV FeII emission, but weaker optical FeII emission.

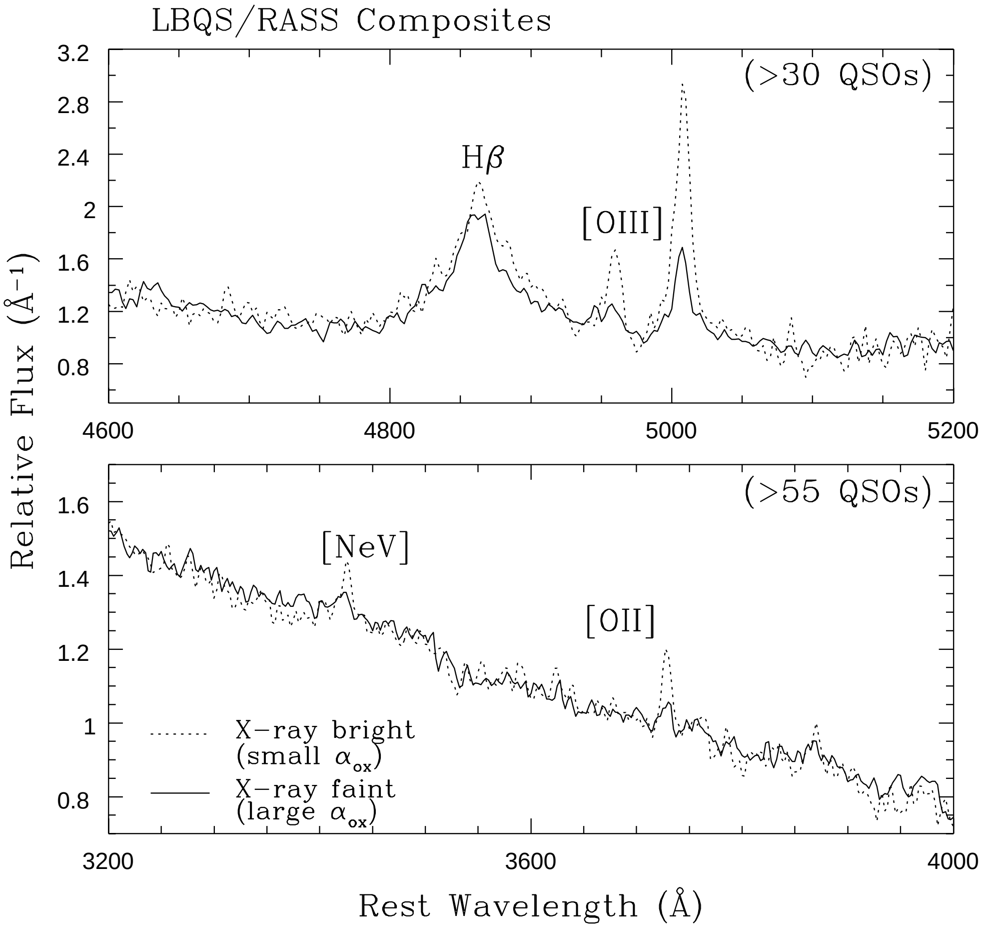

Figure 3. Normalized restframe composite spectra of the LBQS/RASS sample (Green 1998). In this plot, the X-ray bright composite spectrum (dashed lines) is overlaid on the X-ray faint composite spectrum (solid lines). The upper plot highlights the region around Hβ, while the lower plot shows the enhancement of even the weaker narrow forbidden lines in the X-ray bright composite. The minimum number of QSOs whose spectra contribute at every wavelength is shown in the upper right hand corner.

Of the emission lines to which we can fit two components (Lyα, CIV, MgII, and Hβ), Hβ is the *only* line for which the percentage of total line flux in the narrow line component may be *larger* in the XF composite. Since Hβ appears to be unique among the larger variety of emission lines studied here, it is clear that it may not be the best, or only representative of BLR line widths. Fitting the Hβ line in our optical composites with a *single* Gaussian component leads to similar conclusions to previous studies (i.e., that FWHM(Hβ) is larger in

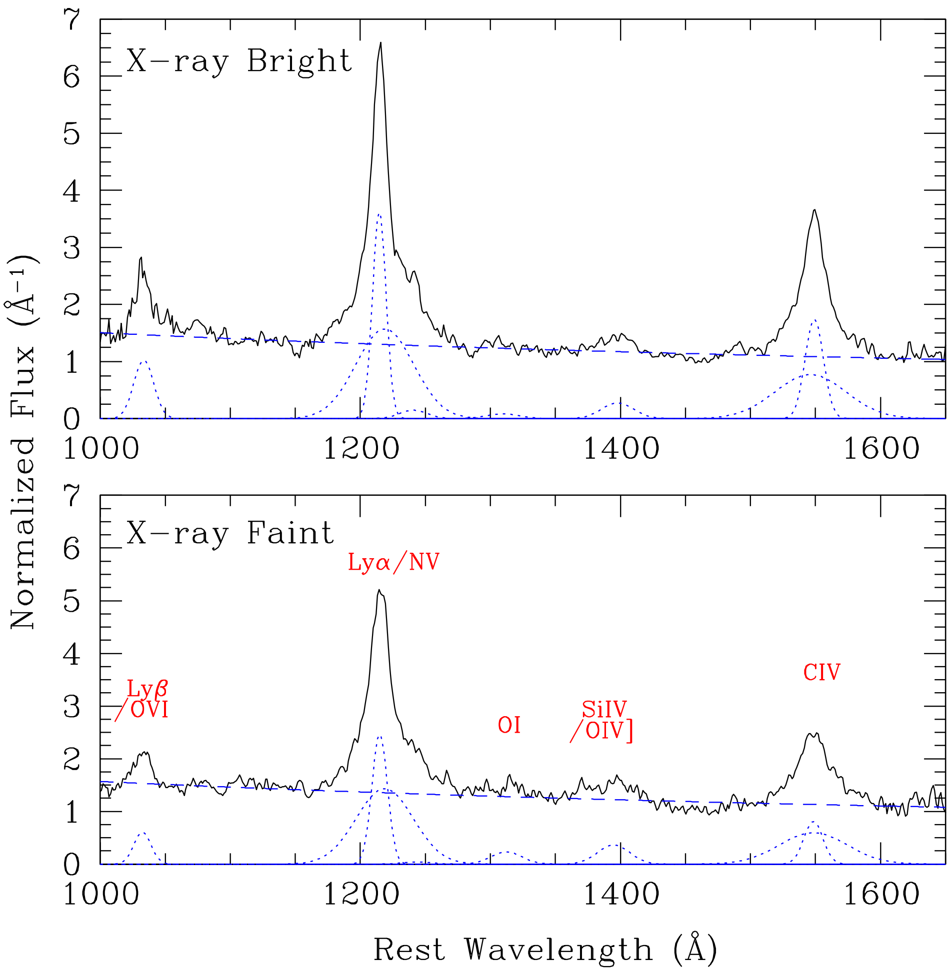

Figure 4. Normalized restframe composite spectra of an IUE/Einstein sample (Green 1998). The top plot is the X-ray bright composite, and the bottom shows the X-ray faint composite. The best-fit components are shown in each plot: a powerlaw continuum (dashed line), fit simultaneously with Gaussian emission lines (dotted lines).

the XF composite; Laor et al. 1997, Boroson & Green 1992). However, fitting narrow and broad line components separately reveals that Hβ has a stronger broad component in the XB composite, and a larger broad/narrow line ratio, while the actual FWHM is similar to the XF composite. This reveals that single Gaussian fits to compound lines must be interpreted with caution.

This direct evidence shows that SEDs (at least as crudely represented by α_{ox}) strongly affect line emission in the correct sense to account for the BEff. However, all 5 mechanisms mentioned - orientation, variability, optically thin clouds, covering fraction, and SED shifts are likely to play a role. Occam's razor demands that we seek the most economical description of the data.

5. Can Trends with α_{ox} Alone Account for the BEff?

The observed trends just illustrated of W_λ with α_{ox}, combined with the trend of α_{ox} with luminosity might account for the BEff. Removing α_{ox} from these observed trends allows us to crudely check if the effect of α_{ox} on emission lines can fully account for the observed slope of the BEff.

From Green et al. (1995) or Wilkes et al. (1994), $\alpha_{ox} \sim 0.11 \log L_{opt}$. Dividing the changes in W_λ between the XB and XF composite spectra by the difference between their mean α_{ox} yields a direct relation between α_{ox} and W_λ. Eliminating α_{ox} then yields

log W_λ(CIV)$\sim -0.05 \log L_{opt}$, and

log W_λ(MgII)$\sim -0.03 \log L_{opt}$.

By contrast, the slopes of the BEff from Zamorani et al. (1992) for these ions are -0.13 and -0.68, respectively. A simple change in α_{ox} thus seems insufficient to account for the entire BEff. Zheng, Kriss, & Davidsen (1995), taking advantage of the improved S/N and resolution of HST FOS spectra, reported a significant decrease in W_λ(OVI) with α_{ox}. The increase in α_{ox} with luminosity in QSOs when combined with the observed BEff was an insufficient explanation there as well. We note, however, that in all these studies, not only does scatter dominate the regressions, but α_{ox} is only a very crude measure of SED changes. Furthermore, as we will discuss below, the observed SED may not be the same as what impinges on the emission line clouds. Accounting for the BEff with an SED model probably also requires invoking at least one of the other mechanisms. However, that phrase, "invoking at least one of the other mechanisms" may now ring familiar, since it has concluded discussion of each of the 5 mechanisms so far!

6. Extrinsic Effects on the Observed SEDs

Not only is α_{ox} a crude measure of SED changes, worse yet, its observed trend with luminosity has been challenged on several fronts as not reflective of intrinsic properties.

1) **Restframe bandpass.** At higher redshifts, where most of the high luminosity objects are, the soft excess shifts out of the observed soft X-ray bandpass, leaving only the powerlaw component. For radio quiet QSOs, a spectral flattening with redshift is confirmed up to $z \sim 2$ (Yuan et al. 1998a), beyond which the spectral slopes seem to be independent of redshift, similar to that found for radio-loud quasars. This apparent decrease in observed-frame X-ray emission could produce the apparent $\alpha_{ox}(L_{opt})$ correlation. However, this may be a

red herring, since partial Spearman Rank statistical analyses find the primary correlation of α_{ox} to be with L, not z.

2) **Photometric Errors and Intrinsic Dispersion.** LaFranca et al. (1995) argue that errors in L_{opt} have been underestimated in optically-selected samples, and that proper account of this (including e.g., photometric errors, variability and optical spectral slope) destroys the significance of the $\alpha_{ox}(L_{opt})$ correlation. In a similar vein, Yuan et al. (1998b) claim that an *intrinsically* larger dispersion in L_{opt} than in L_x, combined with observed luminosity functions and typical survey flux limits, is sufficient to create an observed correlation (Figure 5).

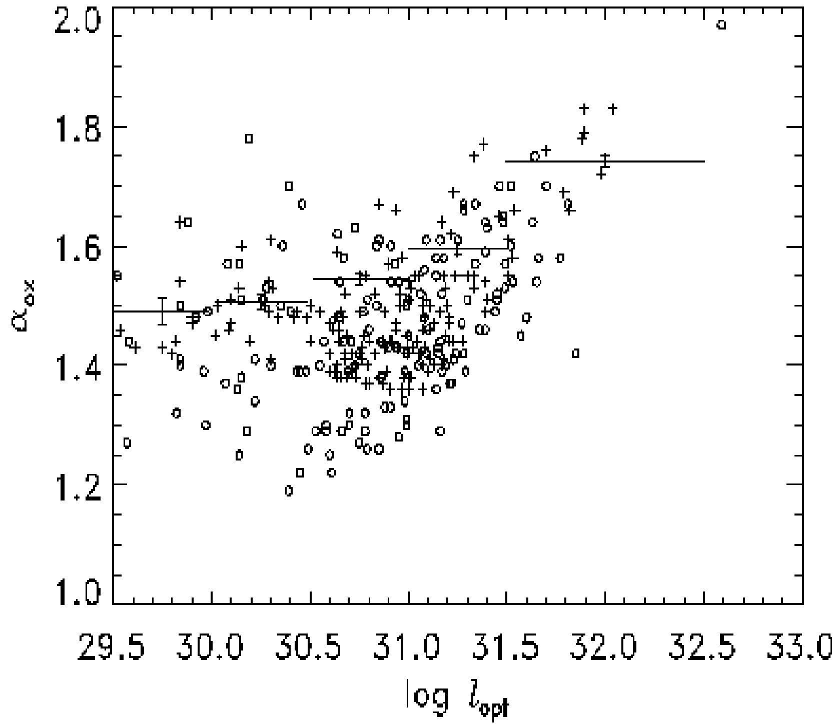

Figure 5. This shows α_{ox} vs. $\log L_{opt}$ for a simulated quasar sample with $0.2 < z < 3$, assuming assuming an intrinsic dispersion 5 times larger in L_{opt} than in L_x (Yuan et al. 1998b). Crosses are non-detections - fluxes below the adopted X-ray flux limit. Horizontal bars show the best estimates of mean α_{ox} in 5 bins of L_{opt}, taking non-detections into account.

Even the more unflappable reader's feathers should ruffle to note that the BEff itself has a structure similar to this α_{ox} vs. $\log L_{opt}$ correlation (Yuan et al. 1998b). The ensemble BEff might be induced if the intrinsic dispersion of L_{opt} exceeds significantly that of line luminosity in QSO samples. Simulations incorporating realistic detection thresholds are needed. Even more importantly, bright volume-limited QSO samples must be conservatively constructed independent of emission line of UV luminosity to avoid these selection-based criticisms.

Deep optical followup of serendipitous sources from AXAF, with its low background and high spatial resolution, offers a unique capacity to do this.

3) **Absorption.** Some of the α_{ox} vs. logL_{opt} correlation could be caused by changes in absorption along the line of sight to the nucleus as a function of luminosity/redshift. In terms of the extinction by cold gas and dust in visual mags, $\tau_B \sim 1.2\ A_V$ and $\tau_{1keV} \sim A_V/2$ (Masci 1998). Therefore, *decreased* cold absorption at higher luminosity would create an accompanying increase in α_{ox}. On the other hand, *warm* (ionized) absorbers can quench X-ray emission without having any detectable effect on the optical, so that *increased* warm absorption at higher luminosities might create the trend. We investigate this further below.

7. Warm Absorption

At a given (optical/UV) luminosity, the strength and profile of many lines appears to depend strongly on the *shape* of the ionizing continuum, even as crudely characterized by α_{ox} (Green 1998). This suggests that SEDs and emission line properties are directly related. Eventually, X-ray emission might be reliably predicted through study of optical/UV emission lines. However, a direct relationship between W_λ and α_{ox} might be mediated by some third parameter characterizing the QSO physics. One such possibility is absorption.

Warm ionized absorbers are a general phenomenon in low luminosity AGN, both in the UV (Crenshaw 1997) and in the X-ray (Reynolds 1997; George et al. 1998). The nearly ubiquitous association of the two (Crenshaw 1997) strongly suggests that they are physically related. For many objects, constraints from both UV and soft X-ray absorption have been applied, yielding physical parameters consistent with the UV/X-ray absorbers being identical (e.g., Mathur, Wilkes, & Elvis 1998). Clouds along the line of sight producing UV absorption lines need not always create X-ray absorption, but X-ray absorbers do produce high ionization UV absorption (Mathur 1997).

Perhaps even in the presence of extrinsic effects such as absorption along the line of sight, emission lines can be used to infer the strength and shape of the high energy SED (Krolik & Kallman 1988, Zheng 1991). As an example, radio-quiet QSOs with broad UV absorption lines (BALs) are now known to exhibit markedly weak X-ray emission as a class (Green et al. 1995, Green & Mathur 1996), and remain mostly undetected. The similarity of emission-line properties in BAL and non-BAL QSOs (Weymann et al. 1991) has been cited as evidence that a chance line-of-sight through a BAL cloud is the cause of the BAL phenomenon and that *all* radio-quiet QSOs have such clouds. If similar emission lines indeed vouch for similar intrinsic high energy SEDs, then the large observed α_{ox} values for BALQSOs are likely to be caused by strong absorption along the line-of-sight rather than by differences in their intrinsic SEDs. This implies that *we often do not observe the same SED that the BELR sees.* The high polarization seen in $\sim 20\%$ of BALQSOs (compared to $\sim 1\%$ in non-BALQSOs) (Goodrich & Miller 1995) strongly suggests that at least those BALQSOs must have an attenuated direct view of the continuum along our line of sight.

Is it plausible that the $\alpha_{ox}(L_{opt})$ correlation is itself caused by absorption? The hypothesis can be tested by removing *all* types of absorbed QSOs - those with known broad or narrow-line intrinsic, damped Lyα, and Lyα forest ab-

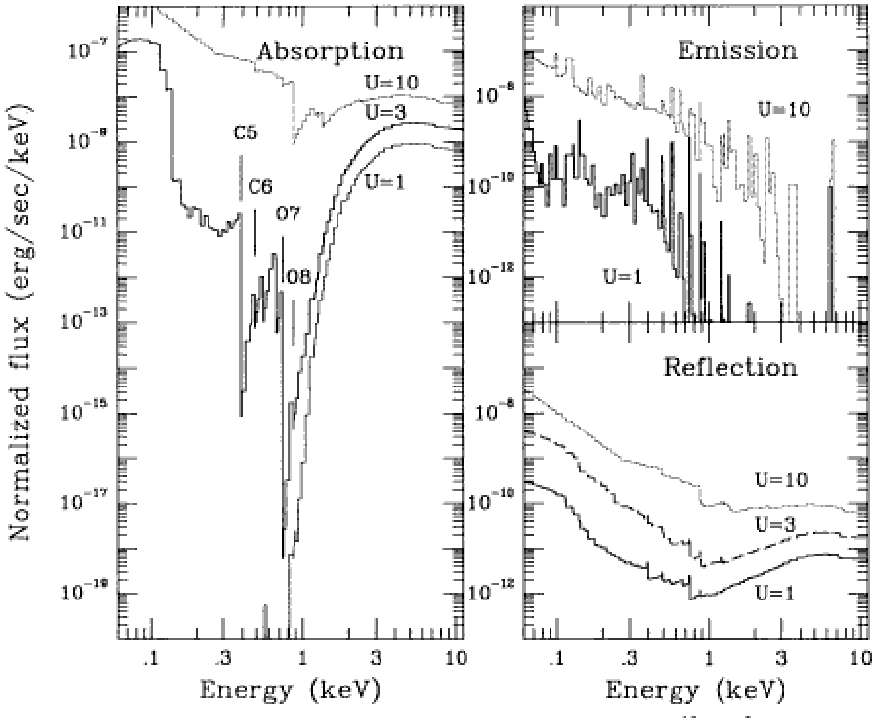

Figure 6. Simulated restframe absorption, emission and reflection spectra of photoionized gas with density $n = 10^{10}\mathrm{cm}^{-3}$ and column density $N = 10^{23}\mathrm{cm}^{-2}$ when exposed to 3 different input ionizing continua (Netzer 1993). The curve at ionization parameter $U = 1$ shows the effects of a neutral absorber. Most significantly, increasing ionization lowers absorption, but it also increases emission and reflection.

sorbers. We performed a cheap version of this test on the QSO sample of *Einstein* pointings in Wilkes et al. (1994; from Table 6). We excluded all QSOs with the following designations as listed in of Hewitt & Burbidge (1993): BALs, known or suspected; UV or 21cm absorption; damped Lyα absorption; any other absorption with or without measured redshifts. We thus reduce the full sample of 514 QSOs to 394 by exclusion of known absorbers (which include about a dozen known BALs), and perform survival analysis (ASURV) regressions on the data. Slopes as measured by both the parametric EM or Buckley-James regressions change by only about 0.01 (only a 1σ difference given the fit errors). One difficulty with this sample is that the optical data are very heterogeneous, as are the absorption IDs. The excluded QSOs are all at the high luminosity side of the distribution, probably because the Lyα absorbers are found toward higher redshifts only.

Our results put no strong constraints on the hypothesis that the $\alpha_{ox}(L_{opt})$ correlation might be due to absorption. Higher S/N samples that have been systematically searched for absorption in both UV and soft X-ray spectra is vastly preferable. We are constructing such a sample from the HST FOS and ROSAT public archives, and will study these issues in an upcoming paper.

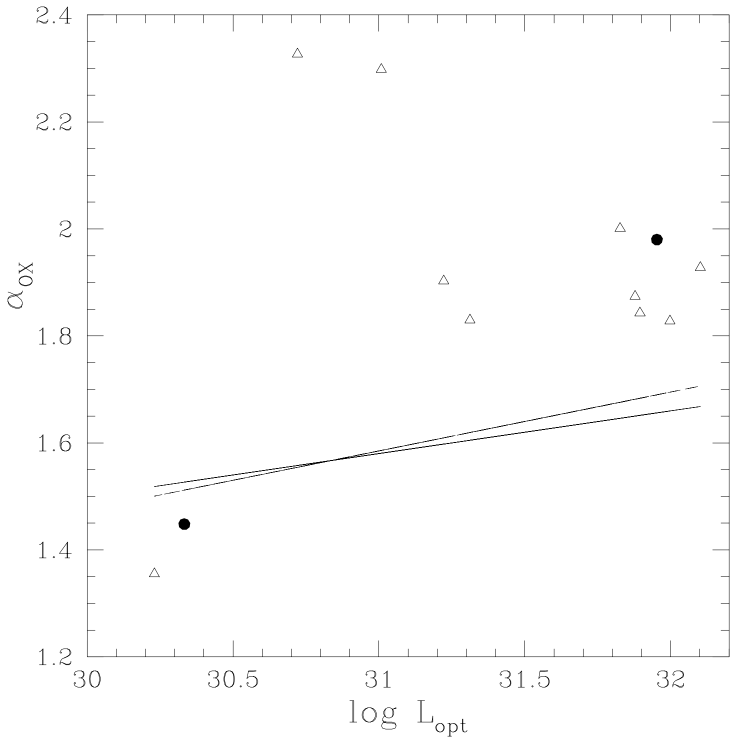

Figure 7. Relative soft X-ray brightness α_{ox} plotted against optical luminosity (Green (1997). The lines are mean regressions to large samples of QSOs, which illustrate the trend of weakening X-ray emission toward higher luminosity. The points are ROSAT PSPC measurements (filled circles) or non-detections (open triangles) of BALQSOs from Green & Mathur 1996. The only detection that appeared to be X-ray bright relative to normal QSOs, PG1416-129, turns out to have been misclassified, and is not a BALQSO (Green et al. 1997).

If at least some of the $\alpha_{ox}(L_{opt})$ correlation is caused by increased warm absorption at higher luminosities, then the correlation would be expected to be weak in soft X-ray selected samples. More common absorption in the UV bandpass is suspected at higher luminosities, but remains to be demonstrated statistically. In the X-ray bandpass, the same charges have been leveled at the popular assumption that absorption is *less* common at high luminosity (Malizia et al. 1997). This latter notion should be particularly suspect, since in most high luminosity objects, higher energy rest-frame X-ray emission is observed, which requires a higher intrinsic absorbing column for detection. Furthermore, the most luminous objects in samples to date have also been radio-loud (Reynolds 1997), while $\sim 90\%$ of QSOs are radio-quiet.

8. Cold Absorption

Seyferts with warm absorbers tend to have higher polarization P (see Figure 8), probably due to dust transmission or scattering of the continuum. Since $P_{continuum} > P_{BELR} > P_{NELR}$, the scattering material is interior to the NELR (Leighly et al. 1998). This point is important to remember, since it indicates a possible association with the molecular torus.

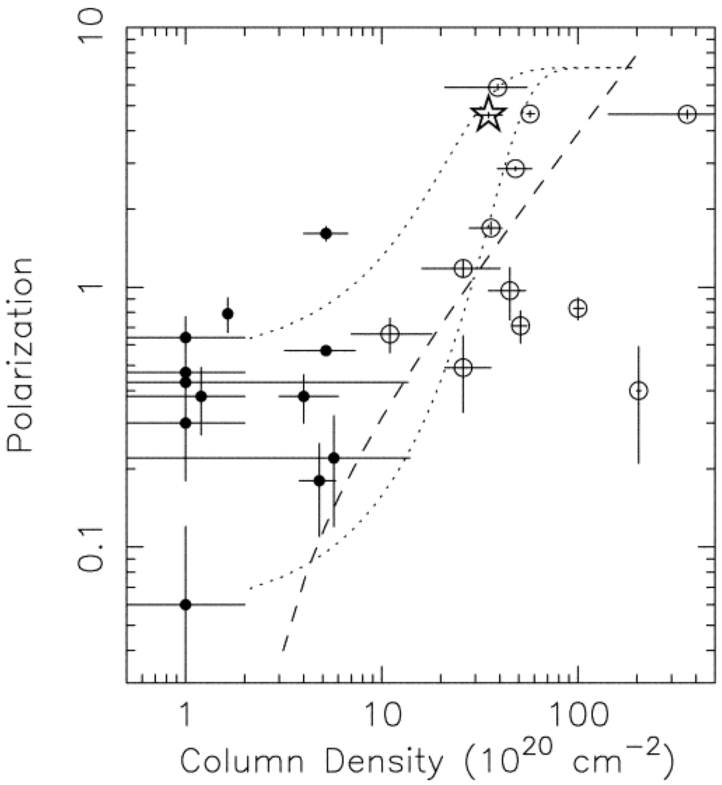

Figure 8. Absorption column density versus polarization (Leighly et al. 1998). Ionized absorber column density in objects where warm absorption provided a good fit to ASCA spectra are shown as open circles. For objects with cold absorption a better fit, filled circles plot the excess over Galactic column. High optical polarization objects are very likely to have warm absorbers.

Optical reddening is seen in some AGN that also have warm absorbers. This can be reconciled with the bright soft X-ray emission if the ionized gas also harbors dust (Brandt et al. 1996, for the quasar IRAS133492438). Such an association of the warm absorbers with dust was shown in larger samples by Reynolds (1997) and Grupe et al. (1998).

Moderate amounts of cold gas and dust are sufficient to explain correlations between continuum slopes seen in the soft X-ray selected AGN sample of Puchnarewicz et al. (1996, 1998). This aesthetically disturbing hypothesis suggests that correlations are caused by absorption, while *intrinsic* SED (and redshift) differences account for the scatter.

9. X-rays and FeII Emission

QSOs with large α_{ox}, of which BALQSOs represent an extreme, have not only weak [OIII], but feeble narrow line emission in general. These correlations may be an effect of absorption and/or scattering of the intrinsic high energy con-

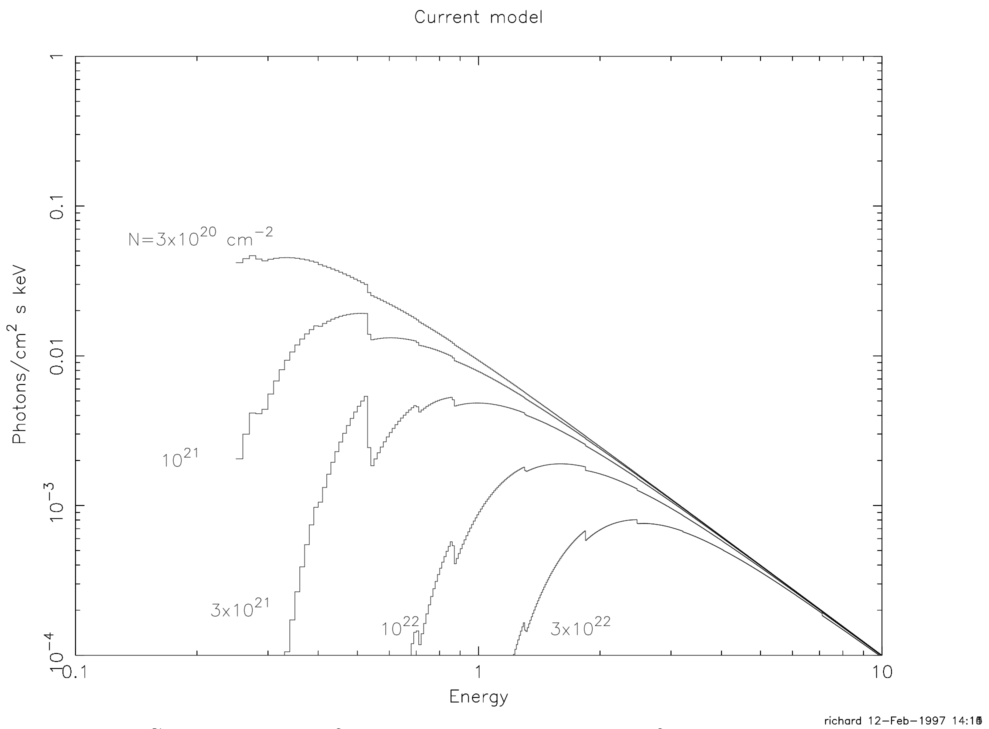

Figure 9. Simulated restframe X-ray absorption of column densities of cold material increasing from $N = 3 \times 10^{20}$ to $3 \times 10^{22}\mathrm{cm}^{-2}$ for an input $\Gamma = 2$ powerlaw continuum (Mushotsky 1997).

tinuum by thick clouds between the BELR and the NELR. The clouds could prevent the ionizing continuum from reaching the NELR (and/or us), but X-ray heating could cause those same clouds to emit copious FeII emission in the optical. This is reinforced by another very strong observed correlation - that BALQSOs, albeit X-ray quiet, are generally very strong optical FeII emitters (Stocke et al. 1992, Lipari et al. 1993). Strong optical FeII emitters in general show large α_{ox} (Lawrence et al. 1997). [8]

Surprisingly, FeII emission in the UV seems to show the opposite behavior. Green et al. (1995) found that QSOs in the LBQS with strong UV FeII emission are particularly bright in the soft X-ray bandpass (Figure 10. LBQS/RASS composite spectra (Green 1998) confirm that X-ray bright (low α_{ox}) QSOs have stronger UV FeII emission.

Lawrence et al. (1997) found that QSOs with strong optical FeII emission can have ROSAT X-ray spectra either flat or steep, while weak optical FeII QSOs always have flat X-ray spectral slopes. In most photoionization models (e.g., Krolik & Kallman 1988), UV FeII originates at low optical depths in BLR clouds where EUV and soft X-ray photons contribute to heating. FeII emission in the optical is principally due to higher energy photons (above $\sim$ 800eV).

[8] Most studies confuse the FeII issue by examining its ratio to Hβ emission, which itself has strong behaviors relative to X-ray brightness.

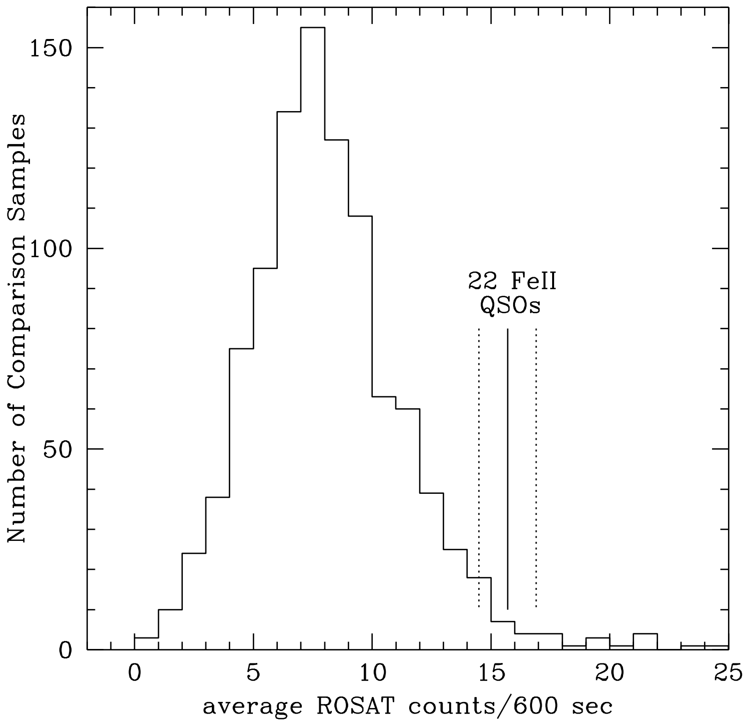

Figure 10. QSOs with extremely strong FeII were selected from the LBQS/RASS sample (Green et al. 1995). ROSAT counts for the stacked FeII QSOs are a factor of 2 higher than the mean for 1000 stacked subsamples of 22 QSOs randomly chosen from 467 non-FeII QSOs in a similar redshift range ($0.4 < z < 1.5$). This occurs only 2% of the time by chance.

But combining theory and observation has generated no *Eureka!* so far. FeII emission is underpredicted by a factor of 4-5 in photoionization models (Wang et al. 1996) and models probably need drastically revised photoionization cross-sections (Bautista & Pradhan 1997 and references therein). Proper modeling of non-radiative heating, optical depth effects, and iron recombination rates, along with improved methods of FeII emission measurements (e.g. Vestergaard 1998) may all be needed to unravel the intriguing observations.

10. We Don't See the SED That the Emission Line Clouds See

It is now established that warm absorption is quite common. Because highly ionized absorbers are more difficult to recognize (see Figure 6), they may be ubiquitous. Cold absorption, albeit with stronger signatures (see Figure 9) could also be much more common than we realize, since historically, QSO studies have been dominated by samples selected in the optical and/or soft X-ray bandpasses. Webster et al. (1995) showed that flat spectrum radio-selected quasars exhibit a much broader range of $B - K$ colors, and claimed that nearly 80% of QSOs might have been missed in traditional surveys.[9]

The glum fact is that, even in extant samples mostly biased *against* absorption, we quite often do not observe the unabsorbed intrinsic continuum. Covering factors of absorbing clouds estimated from existing samples are almost surely underestimates of the intrinsic covering fractions (Krolik & Voit 1998). In upcoming hard X-ray-selected samples, we should expect the discovery of larger fractions of BALQSOs and dust-obscured quasars.

It is also clear that since line-of-sight effects are important, many paths from the nuclear continuum, including particularly those to emission line clouds, are not subject to the same SED that we observe. This is of course consistent with the Seyfert 1/Seyfert 2 unification paradigm (Antonucci 1993, and references therein), but extends to all luminosities. Indeed, since all accretion disk or jet models are intrinsically anisotropic, and since ionization cones observed in AGN (Mulchaey et al. 1996) are in many cases consistent with biconical continuum radiation, we can be assured that this effect pervades observations at all luminosities. By extension, we can also be confident that many emitting clouds do not see the same SED as others, so that geometric effects and self-shielding are also pervasive, and should be accounted for in multizone photoionization models.

A composite soft X-ray SED generated from the 23 QSOs in the UV-selected ROSAT sample of Laor et al. (1997), combined with the HST FOS composite of Zheng et al. (1997) points to a surprisingly weak - or absent - EUV bump.[10] A similar SED (a Comptonized accretion disk, with $f_\nu \propto \nu^{-2}$) fits multiwavelength spectra from Mrk335 (Zheng et al. (1995). A recent analysis of Mrk335 by Korista, Ferland, & Baldwin (1997) shows that given this input SED, not even full coverage by optimally-emitting clouds can produce the observed W_λ(HeII). The HeII-emitting clouds must see a brighter, or harder EUV continuum than we observe.

Across a broad range of AGN type and luminosity, the observed continuum shows a clear deficit of ionizing photons sufficient to produce the observed Hβ emission (Binette, Fosbury, & Parker 1993). Naively, we might invoke anisotropy to mitigate the conflict; we do not observe the same continuum strength as that impinging on the emitting clouds. However, our line of sight to the continuum would *always* have to be outside the collimated radiation cone. Also, since $W_\lambda(H\beta)$ is constant across 5 orders of magnitude in luminosity, a spectacularly fine-tuned fraction of the continuum would have to be scattered in our direction across this range. The ultimate cause of the derived photon deficit is the assumption of a point source origin for the continuum, and a covering fraction $< 10\%$ compatible with the proportion of QSOs showing Lyman limit absorption (e.g., Koratkar, Kinney, & Bohlin 1992; Antonucci et al. 1989). Both these constraints can be alleviated if the continuum may be produced or reprocessed cospatially with the BLR. There is observational evidence for an apparently ex-

[9] Benn et al. 1998, however, attribute such results to a K excess, possibly due to starlight contamination and/or a non-thermal synchrotron contribution in the IR.

[10] However, the blue end of this spectrum near 300Å used to extrapolate to the soft X-ray regime suffers from extremely large absorption corrections.

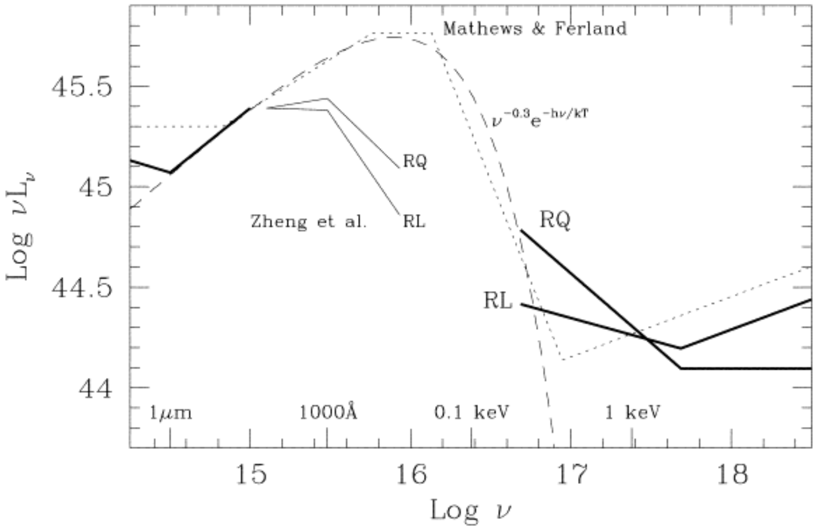

Figure 11. A composite UV/soft X-ray SED for radio-loud and radio-quiet quasars (Laor et al. 1997). Excluded from the mean are X-ray weak quasars, and one with a known warm absorber. The mean spectra were extended above 2 keV assuming a slope of -1 for RQQs and -0.7 for RLQs. The Mathews & Ferland (1987) quasar energy distribution is also displayed for the purpose of comparison.

tended nuclear continuum, and for spatial association of line and continuum, for example from HST (Caganoff et al. 1991).

If the line-emitting clouds in the BELR themselves possess significant electron scattering opacity, several problems are solved at once (Ferland et al. 1992). Short BLR time lags arise naturally since the continuum is produced *in situ*. Scattering broadening might produce part of the BLR line width. Note also that this might explain why the broad component doesn't vary as strongly with continuum as the narrow component in the ensemble BEff. A flattened distribution of such scattering clouds could also contribute substantially to the observed anisotropy by reflecting light toward the poles.

11. Eigenvector 1 and the High Energy Continuum

Since many QSO SEDs may be absorbed, the question of whether similar emission lines are indeed testimony for similar intrinsic SEDs must be answered through the systematic study of line/continuum correlations in *unabsorbed* QSOs. Neutral and slightly ionized absorption is fairly easily recognized. Although the EUV part of the driving continuum will remain largely inaccessible, a reliable determination of the ionizing continuum, at least in the X-ray regime, requires X-ray spectral modeling at good resolution. The low resolution of most X-ray spectra to date has meant that it is usually not possible to directly measure X-ray line and continuum parameters. As a result, X-ray spectral modeling has become rather sophisticated (Figure 6. Components routinely used in modeling now include powerlaws, optically thin thermal plasma, neutral absorption, warm absorption and/or emission with ionization parameter U, and Compton reflection of the primary continuum by optically thick neutral material (George et al. 1998). Any of the absorbing components may be modeled at any intervening redshift, with partial covering and/or scattering.

In a small, uniform sample of optically-selected QSOs (Laor et al. 1997), the strongest correlation found between X-ray continuum and optical emission line parameters was of the soft X-ray spectral slope Γ (where $f_\nu \propto \nu^{-\Gamma}$) and the FWHM of the H$\beta$ emission line. Strong correlations between Γ, $L_{[OIII]}$, FeII/,Hβ and the [OIII]/Hβ ratio were seen both there and in previous QSO studies (e.g., Boroson & Green 1992). The latter authors found that most of the variation in the observed properties of low-redshift QSOs can be represented in a principal component analysis (PCA) by eigenvectors linking FeII, [OIII], Hβ, and HeII emission line properties with continuum properties such as radio loudness, and the relative strength of X-ray emission, as characterized by α_{ox} (see also Figure 3). A recent, and possibly related result is that Seyfert 1s with broad Hβ emission lines tend to have hard (flat) X-ray spectral slopes (e.g., Brandt, Mathur, & Elvis 1997).

Suppose Eigenvector 1 is driven by some physically meaningful parameter. A good empirical crucible in which to test that hypothesis is between BALQSOs and the Narrow Line Seyfert 1s (NLS1s). These two types of AGN are both towards the same extreme of Eigenvector 1 (weak [OIII], strong optical FeII, radio quiet), while the dissimilarity between their high energy SEDs could scarcely be greater. In the soft X-ray bandpass, NLS1s are bright and variable, with steep, soft slopes (Boller, Brandt, & Fink 1996), while BALQSOs are virtually undetectable (Green & Mathur 1996).

The optical emission line characteristics of Eigenvector 1 were proposed by Boroson & Green (1992) to be related to L/L_{Edd}. As this ratio increases, the accretion disk puffs up, increasing the warm ionized (FeII) volume, but blocking much of the radiation from reaching the NELR. For BALQSOs, our line of sight might skim the disk where a radiation-driven disk wind creates high velocity absorption lines (Yamamoto, this volume; Murray & Chiang 1995). For NLS1s, the strong X-ray soft excess and variability could be explained as radiation with relativistic effects from an accretion disk (around a Kerr black hole) also at high inclination to our line of sight (Rauch & Blandford 1994; Sun & Malkan 1989). ASCA spectra show absorption features near 1keV that could be evidence for outflowing warm absorbers in NLS1s (Leighly et al. 1997). If confirmed as such, BALQSOs and NLS1s could be even more closely linked empirically. Efforts are underway at all wavelengths to further investigate the relationship between these objects to determine what the difference is in physics or orientation that precludes in NLS1 the absorption seen in BALQSOs. Theoretically, however, the game may be wide open, since pole-on models exist for both classes.

12. Summary

Line/continuum studies show that the emission lines we see often correlate with the observed SED. Many results are consistent with U decreasing as luminosity increases, i.e., a shift in the SED to lower energies at higher luminosities. Such a trend affects both line and continuum emission in the correct sense to account for the BEff. Photoionization models assuming a distribution of clouds (i.e., not a single U) predict a strong dependence of W_λ on the (assumed powerlaw) slope of the SED (Korista, this volume). However, to account for the bewildering array of line/continuum correlations, many mechanisms other than intrinsic SED shifts - orientation, variability, optically thin clouds, absorption and covering fraction - are likely to play a role.

Unfortunately, we are often not privileged to observe either the SED to which line-emitting clouds are subject, or by extension the intrinsic SED. Fundamental parameters as $\dot{M}$ and M_{BH} determine the luminosity and intrinsic SED, which in turn affects the scale of the BELR. Objects with large α_{ox} based on low-resolution soft X-ray measurements could either have small black holes and high accretion rates, yielding harder spectra, or they could simply be absorbed along our line of sight. The latter does not ensure that the intrinsic SED is absorbed along a path to the NELR, since an interplay of orientation and absorption is often at work. Even when assuming flattened geometries, we cannot as yet assume that the accretion disk, BELR, torus, and NELR are coplanar. Not only is any combination of alignments between these components currently allowable, but alignment of the entire geometric system to the observer's line of sight is also a variable.

Despite all that waffling, we suggest (as have others) that the as yet mysterious physical link between the many diverse properties discussed herein is related to high velocity, outflowing winds near the nucleus that, by absorbing the intrinsic nuclear continuum, strongly affect the radiation observed at larger distances. The continuum impinging on the NLR is most often closest to that received by distant observers like ourselves, but may be quite different from that seen by the BLR. Material in the BLR itself may reprocess the intrinsic continuum issuing from the unshrouded QSO nucleus.

Signatures of optically thin clouds, orientation, and covering factor are fairly difficult to extract, requiring high S/N data and detailed analysis. Variability is perhaps more directly testable, but requires multiepoch spectra, which currently exist only for a handful of objects. Since multiwavelength data exists for many AGN, the SED model remains among the most empirically testable mechanisms for producing the BEff considered here.

The SED model predicts that the luminosity in lines whose driving continuum is cleanly observable will be linearly proportional to that continuum, and thereby show no Baldwin Effect relative to it. Good line candidates should have driving continua in the X-ray bandpass, with no contribution (as with Lyα and CIV) from softer continuum components. Some examples are observationally challenging (e.g., He Iλ5876 is weak; C IIλ326, O Iλ8447, and Ne VIIIλ774 are in difficult wavelength regimes). Study of other lines is more tractable: FeII lines in the UV have their driving continuum above 500eV; FeII lines in the optical are principally due to continuum above 800eV. MgIIλ2798 appears to be an even better candidate for testing these predictions. According to photoionization models, this line has a driving continuum between 600-800eV, and it is more easily measured than are the broad FeII multiplets. Studies of MgII emission lines vs. X-ray continuum appear to have been overlooked. It is essential that we extend these tests across a range of redshifts and luminosities, using high S/N spectra and large, homogeneous samples. Although the production of emission lines is sensitive both to ionization parameter (U, essentially the ratio of photon flux to electron density) and abundance (e.g., Korista et al. 1996), the effects of input SED have so far received less attention.

A multiwavelength approach with particular attention to the interplay of absorption and emission shows promise for significant advances in our understanding, so we are accumulating a high-quality homogeneous database for a large sample of QSOs, primarily from the ROSAT and HST archives.

Acknowledgments. Many thanks to the conference organizers for sponsoring a stimulating and supportive conference. The author gratefully acknowledges support provided by NASA through Grant NAG5-1253, and Contract NAS8-39073 (ASC), as well as through Grant NAG5-6410 (LTSA).

References

Antonucci, R. R. J., Kinney, A. L., & Ford, H. C. 1989, ApJ, 342, 64

Antonucci, R. R. J. 1993, ARA&A, 31, 473

Baldwin, J.A. 1977, ApJ, 214, 679

Baldwin, J. A., Ferland, G., Korista, K., & Verner, D. 1995, ApJ, 455, 119

Barvainis, R. 1993, ApJ, 412, 513

Bautista, M. A., & Pradhan, A. K. 1997, A&AS, 126, 365

Benn, C. R. Vigotti, M., Carballo, R., Gonzalez-Serrano, J. I., & Sanchez, S. F. 1998, MNRAS, 295, 451

Binette, L., Fosbury, R. A., & Parker, D. 1993, PASP 105, 1150

Binette, L., Prieto, A., Szusziewicz, E., & Zheng, W. 1989, ApJ., 343, 135

Boller, T., Brandt, W. N., Fink, H. 1996, A&A, 305, 53

Boroson, T. A., & Green, R. F. 1992, ApJS, 80, 109

Brandt, W. N., Mathur, S., & Elvis, M. 1997, MNRAS, 285, 25

Brandt, W. N., Fabian, A. C., & Pounds, K. A. 1996, MNRAS, 278, 326

Caganoff, S. et al. 1991, ApJ, 377, L9

Crenshaw, D. M. 1997, in Mass Ejection from Active Galactic Nuclei, ASP Conference Series, Vol. 128, eds N. Arav, I. Shlosman, R. J. Weymann, p. 121

Edelson, R. A., Pike, G. F., & Krolik, J. H. 1990, ApJ 359, 86

Elvis, M., et al. 1994, ApJSup, 95, 1

Ferland, G. J., Peterson, B. M., Horne, K., Welsh, W. F., & Nahar, S. N. 1992, ApJ, 387, 95

Ferland, G. F., Korista K., & Peterson, B. M. 1990, ApJ, 363, 21

Ferland, G. F., & Shields, G. A. 1985 in *Astrophysics of Active Galaxies & Quasi-Stellar Objects,* ed. J. Miller (Mill Valley, Ca: University Science Books), p.157

Francis, P. J. 1993, ApJ, 407, 519

George, I. M., Turner, T. J., Netzer, H., Nandra, K., Mushotzky, R. F., & Yaqoob, T. 1998 ApJS,114, 73

Goodrich, R. W., & Miller, J. S. 1995, ApJ, 448, L73

Green, P. J., et al. 1995, ApJ, 450, 51

Green, P. J., & Mathur, S. 1996, ApJ, 462, 637

Green, P. J. 1996, ApJ, 467, 61

Green, P. J., Aldcroft, T., Mathur, S., & Schartel, N. 1997, ApJ, 484, 135

Green, P. J. 1997, in Mass Ejection from Active Galactic Nuclei, ASP Conference Series, Vol. 128, eds N. Arav, I. Shlosman, R. J. Weymann, p. 167

Green, P. J. 1998, ApJ, 498, 170

Grupe, D., Wills, B. J., Wills, D., & Beuermann, K. 1998, A&A, 333, 827

Haardt, F., & Maraschi, L. 1993, ApJ, 413, 507

Halpern, J. P. 1984, ApJ, 281, 90

Iwasawa, K. & Taniguchi, Y. 1993 ApJ Letters, 413, L15

Kaspi, S., Smith, P. S., Maoz, D., Netzer, H., & Januzzi, B. T. 1996, ApJ, 471, L75

Kennicut, R. C. 1990 in *The Insterstellar Medium in Galaxies*, ed. Thronson, H. A., & Shull, J. M.

Kinney, A. L. Rivolo, A. R., & Koratkar, A. P. 1990, ApJ, 357, 338

Koratkar, A. P., Kinney, A. L. & Bohlin, R. C. 1992, ApJ, 400, 435

Korista, K., Ferland, G. & Baldwin, J. 1997, ApJ, 487, 555

Krolik, J. H., & Voit, G. M. 1998, ApJ Letters, 497, L5

Krolik, J. H., & Kallman, T. R. 1988, ApJ, 324, 714 (KK88)

LaFranca, F., Franceschini, A., Cristiani, S, and Vio, R. 1995, A&A, 299, 19

Laor, A., Bahcall, J. N., Jannuzi, B. T., Schneider, D. P., Green, R. F. 1995, ApJS, 99, 1

Lawrence, A., Elvis, M., Wilkes, B. J., Mchardy, I., & Brandt, N 1997, MNRAS 285, 879

Leighly, K. M., Kay, L. E., Wills, B. J.; Wills, D., &

Grupe, D. 1997 ApJ Letters, 489, L137

Leighly, K. M., Mushotzky, R. F., Nandra, K., Forster, K. 1997, ApJ Letters, 489, L25

Lipari, S., Terlevich, R., & Macchetto, F. 1993, 406, 451

Malizia, A., Bassani, L., Stephen, J. B., Malaguti, G., & Palumbo, G. G. C. 1997, ApJS, 113, 311

Masci, F. 1998, PhD Thesis, astro-ph/9808141

Masnou, J.-L., Wilkes, B. J., Elvis, M., Arnaud, K. A., & McDowell, J. C. 1992, A&A, 253, 35

Mathews, W. G., & Ferland, G. J. 1987, ApJ, 323, 456

Mathur, S., Wilkes, B., & Elvis, M. 1998, ApJ Letters, 503, L23

Mathur, S. 1997, in Mass Ejection from Active Galactic Nuclei, ASP Conference Series, Vol. 128, eds N. Arav, I. Shlosman, R. J. Weymann, p. 161

Mulchaey, J. S., Wilson, A. S., & Tsvetanov, Z. 1996, ApJ, 467, 197

Mushotsky, R. F. 1997, in Mass Ejection from Active Galactic Nuclei, ASP Conference Series, Vol. 128, eds N. Arav, I. Shlosman, R. J. Weymann, p. 141

Mushotzky, R. F., & Ferland, G. J. 1984, ApJ, 278, 558

Netzer, H. 1987, MNRAS, 225, 55

Netzer, H. 1993, ApJ, 411, 594

Netzer, H., Laor, A., & Gondhalekar, P. M. 1992, MNRAS 254, 15

Osmer, P. S., Porter, A. C., & Green, R. F. 1994, ApJ, 436, 678

Otani, C. et al. 1996, PASJ, 48, 211

Pogge, R. W., & Peterson, B. M., 1992, AJ, 103, 1084

Puchnarewicz, E. M. & Mason, K. O. 1998 MNRAS, 293, 243

Puchnarewicz, E. M. et al. 1996 MNRAS, 281, 1243

Reynolds, C. S. 1997, MNRAS, 286, 513

Schartel, N., Green, P. J., Anderson, S. F., Hewett, P. C., Fink, H., Brinkmann, W., Trümper, J., Margon, B., & Foltz, C. B. 1996, MNRAS, 283, 1015

Shields, J. C., Ferland, G. J., & Peterson, B. M. 1995, ApJ, 441, 507

Sprayberry, D. & Foltz, C. B. 1992, ApJ, 390, 39

Stocke, J. T., et al. 1992, ApJ, 396, 487

Sun, W.-S., & Malkan, M. 1989, ApJ, 346, 68

Tananbaum, H., Avni, Y., Green, R. F., Schmidt, M., & Zamorani, G. 1986, ApJ, 305, 57

Vestergaard, M. et al. 1998, in preparation

Wamsteker, W. & Colina, L. 1986, ApJ, 311, 617

Wandel, A. 1997, ApJ, 490, 131

Wang, T., Brinkmann, W., & Bergeron, J. 1996, A&A, 309, 81

Webster, R. L., Francis, P. J., Peterson, B. A., Drinkwater, M. J., & Masci, F. J. 1995 Nature, 375, 469

Weymann, R. J. et al. 1991, ApJ, 373, 23 (WMFH)

Wilkes, B., J., Kuraszkiewicz, J., Green, P. J., Mathur, S., & McDowell, J. C. 1998, ApJ, submitted

Wilkes, B. J., Tananbaum, H., Worrall, D. M., Avni, Y., Oey, M. S., & Flanagan, J. 1994, ApJS, 92, 53

Yuan, W., Brinkmann, W., Siebert, J., & Voges, W. 1998a, A&A, 330, 108

Yuan, W., Siebert, J. & Brinkmann, W. 1998b, A&A, 334, 498

Zamorani, G., Marano, B., Mignoli, M., Zitelli, V., & Boyle, B. J. 1992, MNRAS, 256, 238

Zheng, W., Kriss, G. A., Telfer, R. C., Grimes, J. P., & Davidsen, A. F. 1997, ApJ, 475, 469

Zheng, W. et al. 1995, ApJ, 444, 632

Zheng, W., Kriss, G. A. & Davidsen, A. F. 1995, ApJ, 440, 606

Zheng, W. & Malkan, M. A., 1993, ApJ, 415, 517

Zheng, W., Fang, L. Z., & Binette, L. 1992, ApJ, 392, 74
Zheng, W. 1991, ApJ, 382, L55